Efficiently Light-Controlled Reconfigurable Semiconductor Micromotors in Electric Fields

Zexi Liang, Donglei Fan

Abstract—To develop active materials that can efficiently respond to external stimuli with designed mechanical motions is a major obstacle that have hindered the realization nanomachines and nanorobots. Here, we present our finding and investigation of an original working mechanism that allows multifold reconfigurable motion control in both rotation and alignment of semiconductor micromotors in an AC electric field with simple visible-light stimulation. In our previous work, we reported the instantly switchable electrorotation owing to the optically tunable imaginary part of electric polarization of a semiconductor nanowire in aqueous suspension[1]. Here we provide further experimental confirmation along with numerical simulation. Moreover, according to the Kramers-Kronig relation, the real part of the electric polarization should also be optically tunable, which can be experimentally verified with tests of electro-alignment of a nanowire. Here, we report our experimental study of light effect on electro-alignment along with theoretical simulation to complete the investigation of opto-tunable electric polarization of a semiconductor nanowire. Finally, we demonstrate a micromotor with periodically oscillating rotation with simple asymmetric exposure to a light pattern. This research could inspire development of a new class of micro/nanomachines with agile and spatially defined maneuverability.

I. INTRODUCTION

The future micro/nanorobots require a high degree of freedom in motion control to perform complex tasks by individuals or in a swarm. However, in a miniaturized scale, it is a daunting task to apply established actuation approaches used in macroscale robots to micro/nanorobots. Once the dimension of a system is reduced to micro/nanoscale, the complexity in integrating multiple functional components into one structure, resembling those in bulk machines, increases dramatically. However, the level of forces required to drive a robot is dramatically reduced. Interactions that are insufficient for macrorobots become prominent for micro/nanorobots. For instance, interactions between micromotors and external physical fields, including magnetic[2-6], electrical[7, 8], optical[9], and acoustic fields[10] as well as electrochemical reactions[11, 12], have successfully compel versatile motions of micro/nanomotors with strategical material design and fabrication. However, to control the style of motions agilely, efficiently with multifold reconfigurability remains a great challenge[13].

* We are grateful for the support of National Science Foundation via the CAREER Award (Grant No. CMMI 1150767) and research grant EECS-1710922, and Welch Foundation (Grant No. F-1734).

In this work, we first introduce our finding of an innovative working mechanism that can efficiently switch style and modulate speed of mechanical rotation of a semiconductor micromotor in an AC electric field via controlling its optically tunable imaginary part (out-of-phase) of electric polarizability as reported previously. Here, we continue the investigation on the real part (in-phase) of the electric polarization of a silicon nanowire with light exposure and introduce numerical simulation with the consideration of a native oxidation layer of silicon to explain the observed switchable behaviors due to both optically tunable in-phase and out-of-phase electric polarizations. Finally, we demonstrate a micromotor that rotates with periodical oscillation with asymmetric light exposure.

II. RESULTS

A. Materials and Methods

Silicon nanowires with an average diameter of 500 nm are synthesized by nanosphere-templated-metal-catalytic etching [14-16]. In the experiment, a layer of negatively charged nanospheres of 500 nm in diameter is electrostatically assembled on a silicon wafer functionalized with positive charges via layer-by-layer polyelectrolyte coating[17]. Then a Ag thin film is evaporated followed by the removal of the

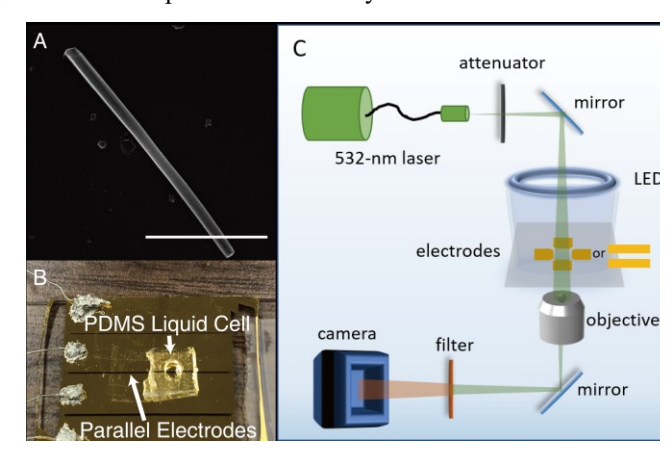


Figure 1. Materials and experimental setup. (A) Scanning Electron Microscopy images of silicon nanowires, scale bar $5~\mu m$. (B) Photo of the parallel electrodews and PDMS liquid cell filled with Si Nanowire suspension. (C) Schematic of the optical-electric setup for reconfigurable manipulation.

Zexi Liang is with the Materials Science and Engineering Program, The University of Texas at Austin, Austin, TX 78712 USA. Donglei "Emma" Fan.is with the Materials Science and Engineering Program, Department of Mechanical Engineering, The University of Texas at Austin, Austin, TX 78712 USA. (e-mail: dfan@austin.utexas.edu).

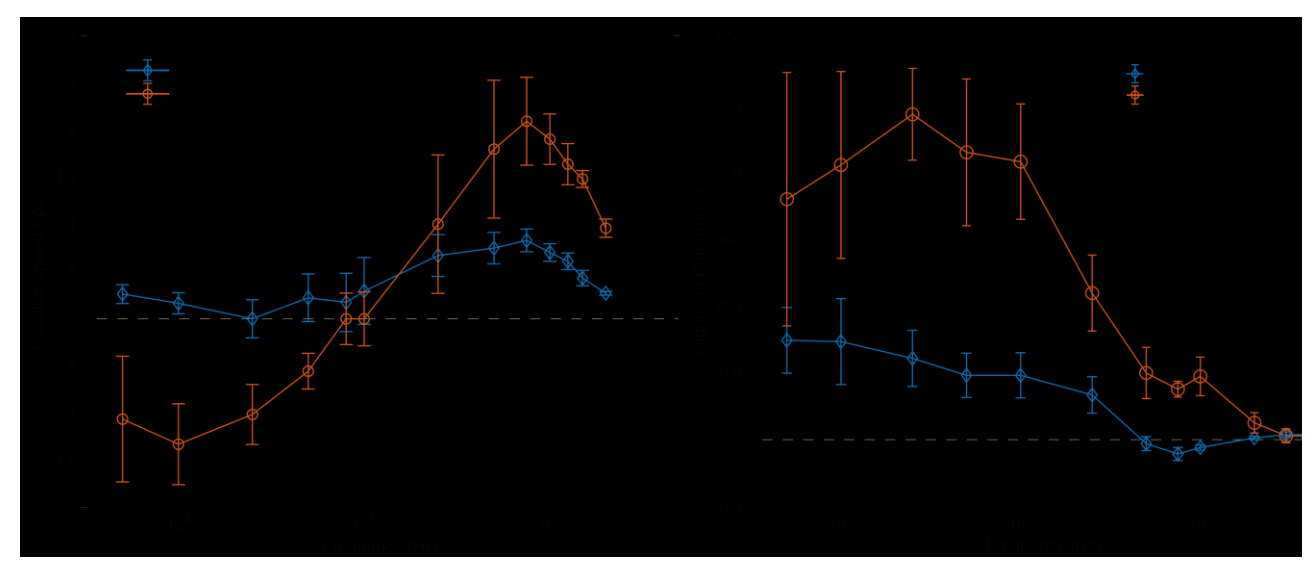


Figure 2. Experimental results of electro-rotation and electro-alignment with and without laser stimuli. (A) Rotation speed (driven by quadruple electrodes) of silicon nanowires (intrinsic 500 nm diameter 10 µm length) versus AC frequency in dim environment and under laser illumination (532 nm). (B) Alignment rate (driven by parallel electrodes) of silicon nanowires (same as in A) versus AC frequency in dim environment and under laser illumination (532 nm).

nanospheres, resulting in a Ag film with arrays of nanoholes. After Ag-assisted catalytic etching in a mixture of hydrofluoric acid and hydrogen peroxide, arrays of Si nanorods can be formed with controlled diameter and length as shown in Fig. 1A.

Two types of microelectrodes are fabricated for the electric manipulation. A quadruple microelectrodes with a gap of 500 μm and a pair of parallel microelectrodes with a gap of 125 μm . The electrodes are made of Au (100 nm)/ Cr (5 nm) thin films patterned on glass slides for rotation and alignment manipulations with electric fields, respectively. In a typical experiment, a microelectrode on glass is placed on an inverted microscope equipped with a 532 nm laser and a customized ring shaped light source providing dim background illuminance (500 lux) (Fig. 1B). Then a nanowire suspension of 20 μl is dispersed into a Polydimethylsiloxane (PDMS) microwell assembled at the center of the microelectrode and are recorded by a CCD camera.

Nanowires can be readily compelled to rotate by an external rotating electric field created via four AC voltages with a sequential 90° phase shift applied on a quadruple microelectrode. The rotation is characterized from 5 kHz to 2 MHz at 20 Vpp at conditions with and without laser illumination. They can also be aligned in the gap of a parallel electrode pair by applying sinusoidal AC voltages of 5 kHz to 4 MHz at 15 Vpp on the parallel microelectrodes. The alignment responses are recorded at different light conditions.

B. Results of electro-rotation and electro-alignment

Agreeing with our previous report [1], we first confirmed the dramatic lighting effects on the rotation of silicon nanowires manipulated in an electric field. The averaged electro-rotation spectra of a separate batch of intrinsic silicon nanowires (5 μ m in length, 500 nm in diameter) with laser illumination at 127 mW/cm² (red curve) and with a background dim light at 500 lux (blue curve) are shown in Fig. 2A.

Here, the positive values of rotation speed indicate the rotation direction is same as that of the electric field. When the light is dim, to just provide sufficient illumination for CCD imaging, the rotational spectrum (blue curve) exhibits consistent co-field rotation in an AC electric field of 5 kHz to 2 MHz with a peak near 100 kHz. When exposure to laser, a reversal of rotation orientation can be immediately observed at frequencies less than 25 kHz as shown in the red curve in Fig. 2A. Moreover, the absolute rotation speeds are substantially increasing across the entire frequency region except that around the co-field to counter field transition at ~80 kHz. The peak frequency of the co-field rotation is shifted to ~500 kHz. Overall, the effect of laser illumination to the rotation spectra of Si nanowires can be categorized into four frequency regions: Region I: from 5kHz to 25 kHz, reversed rotation orientation from co-field to counter-field; Region II: from 25 kHz to 80 kHz, lowered rotation speed; Region III: from 80 kHz to 2 MHz, increased rotation speed compared to the co-field rotation without laser.

Now, with the above experimental analysis, we can readily demonstrate a speed oscillating rotary nanomotor with simple asymmetric light exposure. This can be done by integrating a commercial projector into the microscope system to project designed light patterns onto a single silicon nanowire. Fig. 3 A and B show the snapshots of the long silicon nanowire, partially exposed to a circular light pattern in an electric field of 0.5 MHz AC, 15 V (original video could be found as supplementary materials). When the nanowire rotates to the upper half plane, with less area of light exposure, the rotation is at a low speed state. When the nanowire rotates to the lower half plane with a larger area of light exposure, the rotation is at a high speed state. This light controlled periodic speed modulation suggests a great potential in manipulating nanomotors with complex motions via designing time-dependent light patterns.

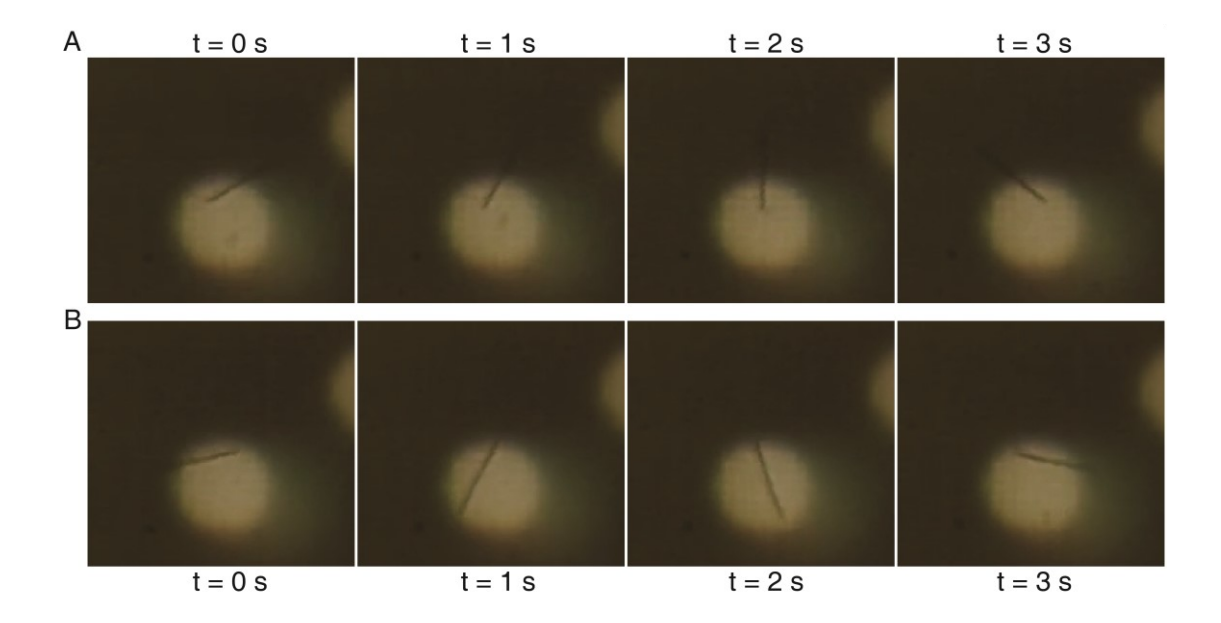


Figure 3. Snapshots of a silicon nanowire asymmetrically exposed to a light pattern from a commercial projector in an AC electric field of 0.5 MHz, 11 Vpp. The nanowire rotates with periodically modulated speed in a single cycle, depending on the area of light exposure. A lower speed in (A) and a higher speed in (B).

Moreover, we find lighting conditions also have remarkable effect on the alignment of silicon nanowires as shown in Fig. 2B. With only minimum background light and no laser exposure, the alignment rate of the nanowire parallel to the external electric field maximizes at 5 kHz, and gradually decreases with the increase of AC frequency. When the frequency hits around 100 kHz, a steep drop of the alignment rate occurs, followed by the perpendicular alignment from 500 kHz to 1 MHz, which is expressed as negative in alignment rates. Then, the reversed alignment returns to the parallel alignment orientation when the frequency of the electric field further increases to ~ 2 MHz at a low rate. When exposed to laser, the alignment rates increase at low frequencies compared to that in dim light. For instance, at 5 kHz, the alignment rate has been increased about 270% from 150 rad/s to 360 rad/s. The maximum alignment rate shifts from 5 kHz to 25 kHz and the value increases over 400%. As the frequency further increases, the alignment rate reduces steeply at around 250 kHz and remains positive till 4 MHz. It indicates that the reversed alignment vanishes in the tested frequency range once exposed to laser. Overall, the laser exposure clearly increases the positive alignment rate at all frequencies, blue-shifts the peak frequency of the alignment spectrum, and diminishes the reversed alignment.

III. ANALYSIS AND MODELING

The experimental studies discussed as above confirm the strong optical responses of semiconductor silicon nanowires in both electro-rotation and electro-alignment. To further understand the interesting while complex phenomena, we conducted theoretical analysis and numerical simulations.

The rotational and alignment torques exerted on a particle arise from the interactions of the electrically polarized microparticle and the applied electric field. Within the limit of low dimension of a particle and approximation of uniform electric field distribution, it is reasonable to apply effective dipole theory to simplify the understanding of the interaction between a polarized particle and the external electric field.[18] Two questions remain: how does the electric field polarize the particle at different frequencies; how does the electric field interact with the induced electric dipole at different frequencies?

A. Effective Dipole Theory

When a uniform AC field is applied, a dipole moment is induced in a nanowire given by $\mathbf{p} = \alpha \mathbf{E}$, where α is the polarizability of the nanowire. To be more specific, the dipole moment can be further decomposed into two different vectors, one is parallel to the long axis of the nanowire, $p_{\parallel} = \alpha_{\parallel} E_{\parallel}$, and the other is along the transverse direction of the nanowire, $p_{\perp} = \alpha_{\perp} E_{\perp}$. The electrical torque exerted onto the dipole is $\mathbf{\tau} = \mathbf{p} \times \mathbf{E}$. Considering the alternating electric field applied in our experiments are above at least 5 kHz, which is a much higher frequency than that of mechanical motions of a typical nanowire, it could be assumed that in one period of the oscillation of the electrical field, the nanowire hardly moves, and thus, the observed torque is actually the time-averaged torque over periods, and can be expressed as[18]:

$$\tau = \frac{1}{2} \operatorname{Re}[\mathbf{p} \times \mathbf{E}^*]. \tag{1}$$

For electro-rotation, the electrical field is circularly polarized and rotates at a same frequency of its oscillation, and the field can be given by $\mathbf{E}(\mathbf{t}) = \mathrm{E}_0 \mathrm{Re}[(\hat{\mathbf{x}} - i\hat{\mathbf{y}})e^{i\omega t}]$, for a counterclockwise rotation. As for the electric alignment, the electric field constantly oscillates along one direction, and can

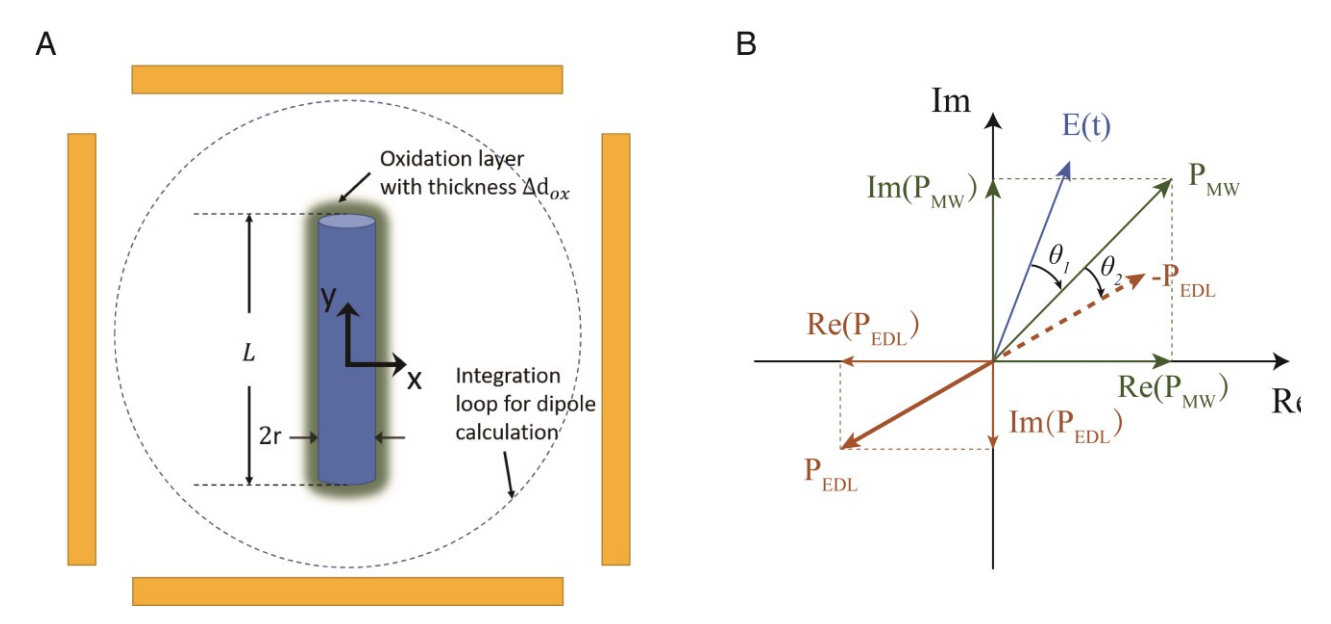


Figure 4. Modeling of nanowire electric polarization and decomposition of the dipole moment. (A) Model of a Silicon nanowire as a cylinder with length L and radius r with an oxidation layer of $\Delta d_{ox} = 1$ nm. (b) Schematic of decomposition of the total dipole moment into real and imaginary components from the Maxwell-Wagner relaxation and the induced electrical double layer effect.

be given by $E(t) = E_0 Re[e^{i\omega t}]\hat{x}$. Taking the expressions of electric fields used in both manipulations into Eq. (1). We can calculate the torques for electro-rotation and electro-alignment, respectively, as follows [19]:

$$\tau_{rotation} = -\frac{1}{2} E_0^2 \text{Im}[\alpha_{\parallel} + \alpha_{\perp}] \hat{\mathbf{z}}. \tag{2}$$

$$\tau_{alignment} = -\frac{1}{2}E_0^2 \operatorname{Re}[\alpha_{\parallel} - \alpha_{\perp}] \sin \theta \cos \theta \,\hat{\mathbf{z}}, \qquad (3)$$

where θ is the angle between the long axis of the nanowire and the electric field.

The Reynolds number (Re) of a typical nanowire is ultralow, i.e. $Re \ll 1$. At such a Reynold number, viscous force dominates the motion. Therefore, the driving electric torque (τ_e) is always instantly balanced by the drag torque (τ_{drag}) as shown by $\tau_e = -\tau_{drag} = \gamma \dot{\theta}$, where γ is the rotational drag coefficient of the nanowire in suspension. For the electro-alignment, the instantaneous speed during alignment is angular dependent and can be expressed by $\dot{\theta} = -A \sin \theta \cos \theta$. Therefore, we investigate the alignment rate given by $A = \frac{E_0^2}{2\gamma} \text{Re}(\alpha_{\parallel} - \alpha_{\perp})$ at different AC frequencies and lighting conditions to understand the optical effect on electric alignment.

B. Frequency Dependent Polarization

The frequency dependent polarization of dielectric materials is known as the dispersion. In optical frequencies, the Lorentz model can well explain the dispersion relation originate from multiple relaxation mechanisms. In our experiment, however, the frequency range of the alternating electric field is much lower and falls in the range of kHz to

MHz, where the dipole, ionic polarization and electronic polarizations are not involved. The only possible polarization mechanism in these frequencies is the interface polarization, also known as the Maxwell-Wagner polarization, which is originated from the discontinuity of the electrical properties at the interface between two mediums. Differ from our previous analytical model with approximation of the nanowire geometry as an ellipsoid, here in this paper, we implement numerical simulation with the commercial finite element method software COMSOL to calculate the Maxwell-Wagner polarization. The nanowire is modeled as a cylinder as shown in Fig. 4A. To be noticed, a 1-nm thick oxidation layer is included in the model that surrounds the entire cylinder to account for the commonly observed natural oxidation layer of silicon nanowire in aqueous solution. This effort is not only closer to the natural chemistry of the nanowire, but also provides results that agrees with experiments better at low frequency regime, where the oxidation layer can play a role as an additional capacitor. The dashed circle is the integration loop to calculate the dipole moment[20]. Note although in previous work, we reported the optical response of electric rotation of Si nanowires and modelled them analytically. Here the modeling is closer to the reality with the consideration of the thin oxide layer, because of which it is done with numerical Besides the effect of Maxwell-Wagner simulation. polarization, due to the existence of ions in aqueous solution, once the nanowire is polarized, the ions of opposite charges are spontaneously attracted towards the polarized surface to counter the surface charge and thus form charge electric layers, the so called electrical double layers. The behavior of the electrical double layer in AC electric field could be very complex. Here we simplify the system with a RC model for qualitative analysis only and the dipole moment contributed by the electrical double layer can be expressed as:

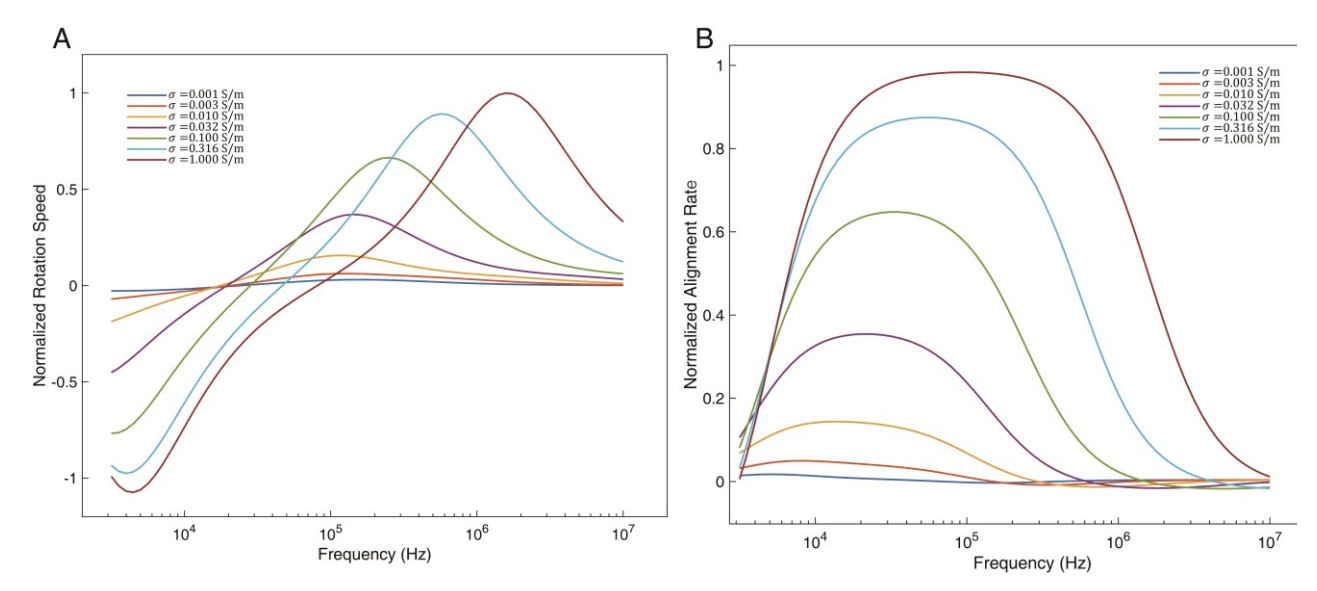


Figure 5. Simulation results of the electro-rotation speed and electro-alignment rate. (A) Simulation of electro-rotation of a nanowire with different electric conductivities versus AC frequency. (B) Simulation of electro-alignment of a nanowire with different electric conductivities versus AC frequency.

$$Im(P_{EDL}) = -\frac{[Re(P_{MW})\sin\delta + Im(P_{MW})\cos\delta]}{\sqrt{\omega^2 \tau_{RC}^2 + 1}}$$
(4)

$$Re(P_{EDL}) = -\frac{[Re(P_{MW})\cos\delta - Im(P_{MW})\sin\delta]}{\sqrt{\omega^2 \tau_{RC}^2 + 1}}$$
 (5)

The synergetic contribution of both the Maxwell-Wagner polarization and the electrical double layer to the total dipole moment of the nanowire is shown in Fig. 4B. Both of the real and imaginary parts of the total dipole moment can be calculated accordingly. In experiments, silicon nanowires are exposed to laser, and thus there will be photo excited carriers generated which lead to additional electrical conductivity termed as photoconductivity. To simulate the laser effect, we sweep the parameter of electrical conductivity of the silicon nanowire in our simulation and get a series of curves for both rotation and alignment rate across the entire frequency range in experiments as shown in Fig. 5A, B respectively. The chosen range of the photoelectric conductivity is adopted from our previous work[1]. With the increase of the electric conductivity, both co-field and counter-field rotation speed increases, and the peak of co-field rotation shift towards higher frequencies in electro-rotation, which agrees well with the experimental result shown in Fig. 2A. For electro-alignment, as the conductivity increases, the alignment rate increases in most frequencies, and the reversed alignment shifts towards higher frequency above the maximum frequency tested in experiments, which could count for the vanishment of the reversed alignment in experiment when laser is on. However, this could also be due to other mechanisms that have not been considered yet.

Overall, our simulation model agrees with the experimental observation qualitatively. It is useful to predict more complex nanostructure's behavior under electrical and optical fields and

may guide the design of semiconductor materials for future applications.

IV. CONCLUSION

In this work, we report an innovative and versatile working mechanism that could be applicable for developing an array of semiconductor based reconfigurable micro/nanomotors, machines, and robots. The electrical property of a semiconductor micromotor can be readily controlled by external light stimuli and is exhibited as modulatable mechanical motion in an external AC electric field. This work could inspire the development a new type of micro/nanomotors with versatile and tempo and spatial adjustable mechanical motions.

ACKNOWLEDGMENT

We thank Dr. Chao Liu, Dr. Kwanoh Kim, Jianhe Guo, Zhengtianye Wang and Daniel Teal for the helpful technical support and discussions.

REFERENCES

- [1] Z. Liang and D. Fan, "Visible light–gated reconfigurable rotary actuation of electric nanomotors," *Science advances*, vol. 4, no. 9, p. eaau0981, 2018.
- [2] Z. Wu *et al.*, "A swarm of slippery micropropellers penetrates the vitreous body of the eye," *Science Advances*, vol. 4, no. 11, p. eaat4388, 2018.
- [3] A. Ghosh and P. Fischer, "Controlled Propulsion of Artificial Magnetic Nanostructured Propellers," (in

- English), *Nano Letters*, vol. 9, no. 6, pp. 2243-2245, Jun 2009.
- [4] J. Giltinan and M. Sitti, "Simultaneous Six-Degree-of-Freedom Control of a Single-Body Magnetic Microrobot," *IEEE Robotics and Automation Letters*, vol. 4, no. 2, pp. 508-514, 2019.
- [5] S. Tottori, L. Zhang, F. Qiu, K. K. Krawczyk, A. Franco-Obregón, and B. J. Nelson, "Magnetic helical micromachines: fabrication, controlled swimming, and cargo transport," *Advanced materials*, vol. 24, no. 6, pp. 811-816, 2012.
- [6] B. Wang *et al.*, "Reconfigurable Swarms of Ferromagnetic Colloids for Enhanced Local Hyperthermia," *Advanced Functional Materials*, vol. 28, p. 1705701, 2018.
- [7] K. Kim, X. Xu, J. Guo, and D. Fan, "Ultrahigh-speed rotating nanoelectromechanical system devices assembled from nanoscale building blocks," *Nature communications*, vol. 5, p. 3632, 2014.
- [8] U. Ohiri, C. W. Shields, K. Han, T. Tyler, O. D. Velev, and N. Jokerst, "Reconfigurable engineered motile semiconductor microparticles," *Nature Communications*, vol. 9, no. 1, p. 1791, 2018/05/03 2018.
- [9] L. Wang and Q. Li, "Photochromism into nanosystems: towards lighting up the future nanoworld," *Chemical Society Reviews*, vol. 47, no. 3, pp. 1044-1097, 2018.
- [10] L. Ren, W. Wang, and T. E. Mallouk, "Two forces are better than one: combining chemical and acoustic propulsion for enhanced micromotor functionality," *Accounts of chemical research*, vol. 51, no. 9, pp. 1948-1956, 2018.
- [11] L. Ren, D. Zhou, Z. Mao, P. Xu, T. J. Huang, and T. E. Mallouk, "Rheotaxis of Bimetallic Micromotors Driven by Chemical—Acoustic Hybrid Power," *ACS nano*, vol. 11, no. 10, pp. 10591-10598, 2017.
- [12] W. Wang, W. Duan, Z. Zhang, M. Sun, A. Sen, and T. E. Mallouk, "A tale of two forces: Simultaneous chemical and acoustic propulsion of bimetallic micromotors," *Chemical Communications*, vol. 51, no. 6, pp. 1020-1023, 2015.
- [13] G.-Z. Yang, P. Fischer, and B. Nelson, "New materials for next-generation robots," *Science Robotics*, vol. 2, no. 10, p. eaap9294, 2017.
- [14] Z. Huang, H. Fang, and J. Zhu, "Fabrication of silicon nanowire arrays with controlled diameter, length, and density," *Advanced materials*, vol. 19, no. 5, pp. 744-748, 2007.
- [15] K. Q. Peng, Y. J. Yan, S. P. Gao, and J. Zhu, "Synthesis of Large-Area Silicon Nanowire Arrays via Self-Assembling Nanoelectrochemistry," *Advanced Materials*, vol. 14, no. 16, pp. 1164-1167, 2002.
- [16] K. Q. Peng, M. L. Zhang, A. J. Lu, N. B. Wong, R. Q. Zhang, and S. T. Lee, "Ordered silicon nanowire arrays via nanosphere lithography and metal-

- induced etching," (in English), *Applied Physics Letters*, vol. 90, no. 16, Apr 16 2007.
- [17] X. Xu, C. Liu, K. Kim, and D. L. Fan, "Electric-Driven Rotation of Silicon Nanowires and Silicon Nanowire Motors," *Advanced Functional Materials*, vol. 24, no. 30, pp. 4843-4850, 2014.
- [18] T. B. Jones and T. B. Jones, *Electromechanics of particles*. Cambridge University Press, 2005.
- [19] García-Sánchez, P., Flores-Mena, J. E. & Ramos, A. Modeling the AC Electrokinetic Behavior of Semiconducting Spheres. *Micromachines*, 10, 100 (2019).
- [20] N. G. Green and T. B. Jones, "Numerical determination of the effective moments of non-spherical particles," *Journal of Physics D: Applied Physics*, vol. 40, no. 1, p. 78, 2006.